

Electroholographic Wavelength Selective Switches in WDM Networks

Aharon J. Agranat.
Department of Applied Physics
The Hebrew University of Jerusalem
Jerusalem 91904, ISRAEL.
Agranat@cc.huji.ac.il ; Tl. 972-2-6584710; Fax 972-2-5610056;

Contents

1. Introduction
2. The electrically controlled Bragg grating.
3. The physical basis of Electroholography.
 - 3.1. The photorefractive effect at the paraelectric phase
 - 3.2. The voltage controlled photorefractive effect in KLTN.
 - 3.3. Assessment of the KLTN crystal as Electroholographic Media
4. The basic switching module.
 - 4.1. The architecture and functionality of the basic electroholography based Switch Module.
 - 4.2. The Performance parameters of the basic electroholography based Switch Module.
5. Applications Electroholographic switching.
 - 5.1. The Electroholographic dynamic optical add drop multiplexer.
 - 5.2. The Electroholographic cross connect.
6. Conclusions.

1. Introduction

The recent years have witnessed an exponential growth of the volume of Internet traffic, accompanied by significant improvements in the performance level and cost effectiveness of the communications technologies. In particular, in optical fiber communication systems, which are the dominant component of the communication infrastructure, these improvements were brought about by two major innovations: the Erbium Doped Fiber Amplifier, and the Wavelength Division Multiplexing (WDM) technology. Both innovations affected primarily the 'long haul' section of the network enabling the data traffic capacity of the backbone of the optical networks to triple every eighteen months. However, the growth rate of the performance of semiconductor devices that are currently used for communication routing has not evolved at a similar rate. Thus, barring a miraculous leap in the performance of silicon, it is clear that the Internet will soon need routing devices that simply cannot be built with the available electronic technology. In order to avoid this projected bottleneck, it is essential to develop an alternative routing technology. In particular, photonic switching where the routing is done in the optical domain is the obvious choice. Substantial effort is currently being devoted to develop a viable photonic switching scheme based on different technologies including microelectronic machining, liquid crystals, integrated optic, and piezoelectric mirrors.

In this paper we describe an alternative generic photonic switching scheme: **Electroholography** (EH). EH is a generic beam steering method based on the voltage controlled photorefractive effect at the paraelectric phase. EH enables the governing of the reconstruction process of volume holograms by means of an externally applied electric field. As will be shown, the application of an electric field on paraelectric crystals in which volume holograms are stored as spatial distribution of a space charge is a necessary condition for the reconstruction of these holograms. Thus, the application of an electric field can be used to activate prestored holograms that determine the routing of data carrying light beams.

The idea of EH was first proposed by Agranat as a generic concept for implementing optoelectronic artificial neural networks (REF1). It was later extended as a generic method for spatial light modulation (REF2). Indeed, the first demonstration of the EH concept was in the form of the EH neuron by Balberg, Agranat et al. (REF3). It was followed by a demonstration of a multistates EH based switch and its use for the implementation of parallel multistage interconnection networks by Pessach, Agranat et al. (REF4).

It is henceforth argued that the concept of EH forms the basis for a *wavelength selective* photonic switching scheme, and as such is particularly suitable for routing in WDM networks.

2. The Electrically Controlled Bragg Grating

The basic building block of electroholographic wavelength selective switching is the electrically controlled Bragg grating (ECBG) as presented schematically in Figure 1. When the electric field is off the grating is in its latent state. In this state (Figure 1a), the grating is transparent so that the incident lightwave propagates through the grating unaffected. When the electric field is turned on (Figure 1b), the grating is activated.

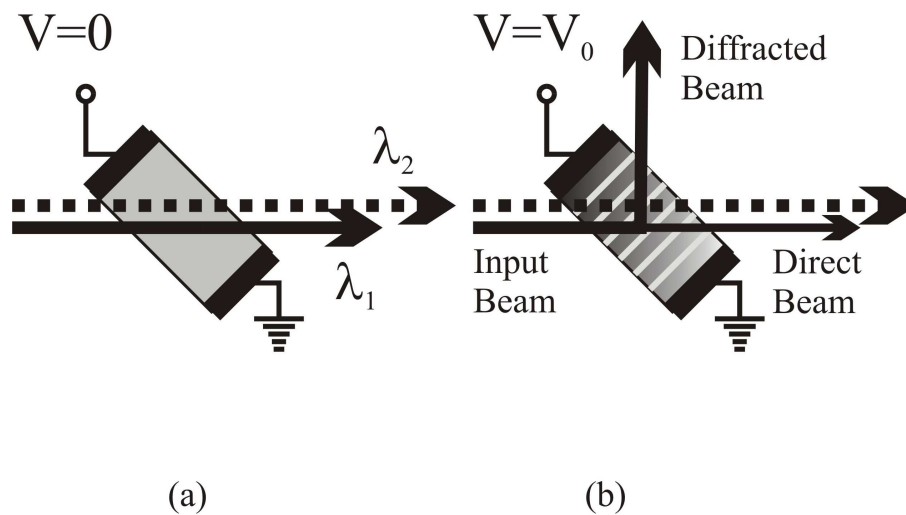


FIGURE 1. The electrically controlled Bragg grating: (a) In the latent state; (b) In the active state.

In the 'on' (active) state an input beam will be diffracted provided it fulfills the Bragg condition (the beam at wavelength λ_1 in Figure 1b). An input beam that does not fulfill the Bragg condition will propagate through the active grating unaffected (the beam at wavelength λ_2 in Figure 1b). Thus, electrically controlled gratings possess the basic features for functioning as wavelength selective switches.

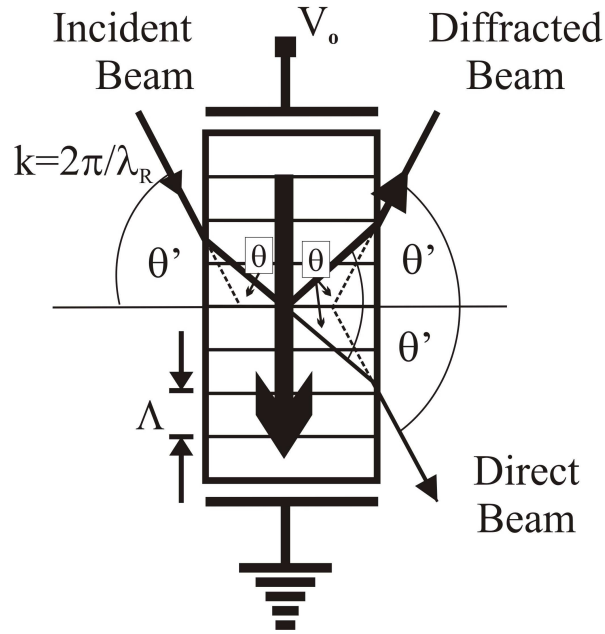


FIGURE 2. A Detailed description of the electrically controlled Bragg grating in the transmission symmetrical configuration.

In order to assess the functions that can be implemented by an electrically controlled grating, consider an ECBG in the transmission configuration as presented schematically in Figure 2. Assume first that the Bragg grating in Figure 2 is passive, namely it is a grating of fixed refractive index modulation and period. The behavior of light beams propagating through a medium with periodic modulation of the (complex) index of refraction is derived from the coupled wave theory of Kogelnik (REF5). (A concise and methodological presentation of the coupled wave theory was published by Solymar in reference 6). Assume that the refractive index in the medium with the imprinted grating is given by

$$n = n_0 + \delta n \cos(Kx) \quad [1]$$

where n_0 is the refractive index of the medium in which the grating was imprinted, δn is the amplitude of the Bragg grating, and K is the grating vector, assumed co aligned with the x axis so that the equiphase planes of the grating are perpendicular to the medium surface. A light beam incident on the grating surface at an angle θ_B (given inside the medium) will be diffracted at an angle $-\theta_B$ provided it fulfills the Bragg condition given by

$$2 n_o \Lambda \sin \theta_B = \lambda \quad [2]$$

where λ is the wavelength of the light in the vacuum, and Λ is the period of the grating (namely: $\Lambda=2\pi/|\mathbf{K}|$). The efficiency of the diffraction when the Bragg condition is satisfied is given by

$$\eta_{\text{diff.}} = \sin^2(\kappa) \quad [3]$$

where η is defined as the ratio between the intensities of the diffracted beam and the input beam respectively, and κ is the coupling constant given by

$$\kappa = \frac{\pi \delta n d}{\lambda \cos \theta_B} \quad [4]$$

where d is the thickness of the grating. If the input beam does not fulfill the Bragg condition [2], the diffraction efficiency is given by

$$\eta_{\text{diff.}} = \frac{\sin^2(\xi^2 + \kappa^2)^{1/2}}{1 + \xi^2 / \kappa^2} \quad [5]$$

where ξ is the Bragg detuning factor given by

$$\xi = \delta\theta \beta d \sin \theta_B \quad [6]$$

in terms of $\delta\theta$ is the angular deviation from the Bragg angle θ_B , and $\beta=2\pi n_o/\lambda$ the wave propagation factor inside the prism.

Assume now that the refractive index in the medium depends on the external field E applied to the medium, and is given by

$$n(x) = n_o(E) + rE \cos(Kx) \quad [7]$$

The application of the field transforms the grating from a latent state in which $\delta n=0$, to an active state in which $\delta n \neq 0$. In the former state $\eta=0$, hence an incident beam continues in its original direction unaffected regardless of its wavelength. In the latter state an incident beam that fulfills the Bragg condition [2] will be diffracted with efficiency η given by [3], whereas an input beam that deviates substantially from the Bragg condition will not be diffracted. Thus, a single ideal ECBG possesses in principle the basic feature of a wavelength selective switching device. Two points however must be addressed up front: (i) The application of the external field affects the constant component of the index of refraction n_0 as well. This fact should be taken into account when designing the operation envelope of the switch as it affects the Bragg condition. (ii) Normally, the ECBG switches less than 100% of the input power. This is due to imperfections in the grating, and the fact that the $\eta=100\%$ is a singular point of the applied voltage where $\kappa=\pi/2$. Therefore a residual fraction of the input power continues in the original direction even when the grating is activated and may cause cross talk between different data channels.

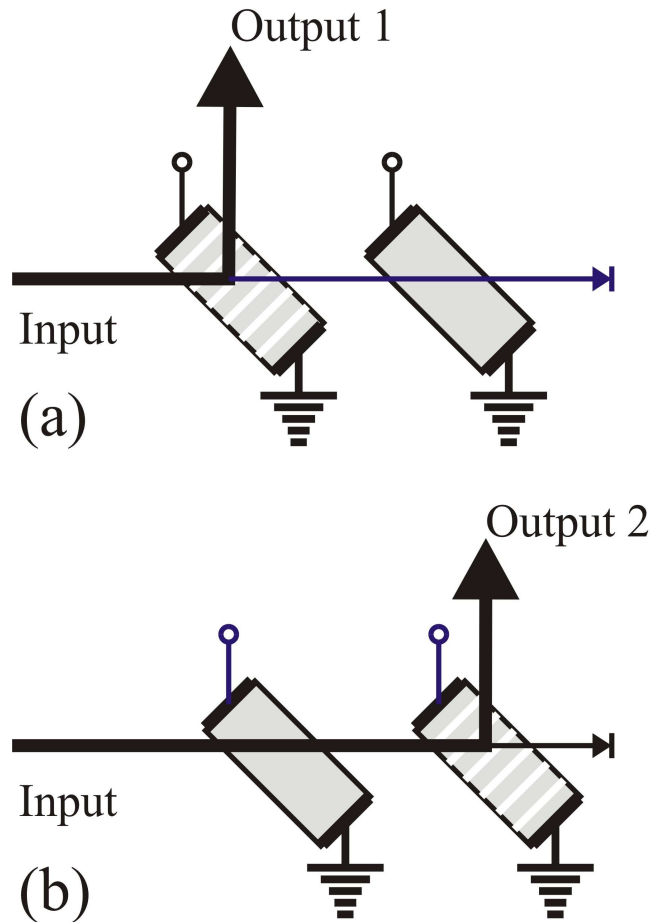


FIGURE 3. A schematic description of a 1x2 electroholographic switch. (a) State 1: the input is connected to output 1. (b) State 2: the input is connected to output 2.

The latter limitation is completely obviated when more than one ECBG is used in the switching device. Consider Figure 3 presenting a schematic description of a 1x2 switch. The switch is constructed of two ECBG that are placed in series along the optical axis of the input beam. When the external field is applied to the first grating (Figure 3a), this grating is activated causing the diffraction of the input beam to emerge out of output 1. Similarly, when the external field is applied to the second grating (Figure 3b), the beam is diffracted off the second grating and emerges out of output 2. Several generic properties of the ECBG switch should be noted

- In both states of the switch the output beam is a diffracted beam, hence the residual power that remains in the direct beam does not cause cross talk. This residual power can be used to monitor the switch without interfering with its operation.

- The applied electric field governs the power of the diffracted beam. Therefore the basic switching operation that is implemented by the ECBG is an analog operation. This fact enables the integration of power management function in the switch fabric itself.
- By governing the applied electric field to both ECBGs simultaneously, the power of the direct beam can be distributed between the two outputs. This property will be exploited later to provide multicasting capability.

In the next two sections the physical mechanism used for implementing the ECBG in photorefractive materials at the paraelectric phase will be presented.

3. The Physical Basis of Electroholography

3.1 The Voltage Controlled Photorefractive Effect at the Paraelectric Phase

The term PR effect is used to describe the phenomena related to the light induced creation of spatial changes in the refractive index. It is normally attributed to the formation of a metastable space charge that is spatially correlated with the incident illumination, and induces changes in the index of refraction through the electrooptic effect. Thus, the PR medium is electrooptic and contains a layer of traps that are partially populated. (*e.g.* iron impurities in LiNbO_3 in which the Nb^{+5} ion is substituted by the Fe^{+3} and Fe^{+2} ions, serving as the empty and populated traps respectively). A qualitative description of the photorefractive process, which leads to the formation of a sinusoidal index grating, is presented in Figure 4.

Two plane waves interfere in the photorefractive medium creating a sinusoidal interference pattern (Figure 4a). This causes photo-ionization of the populated traps, and consequently a generation of free charge carriers at a rate that is spatially correlated with the interference pattern (Figure 4b). The free charge carriers are then transported by diffusion, drift or the bulk photovoltaic effect, and are eventually retrapped by the empty traps. The outcome of this process is a trapped space charge that is spatially correlated with the exciting illumination interference pattern (Figure 4c).

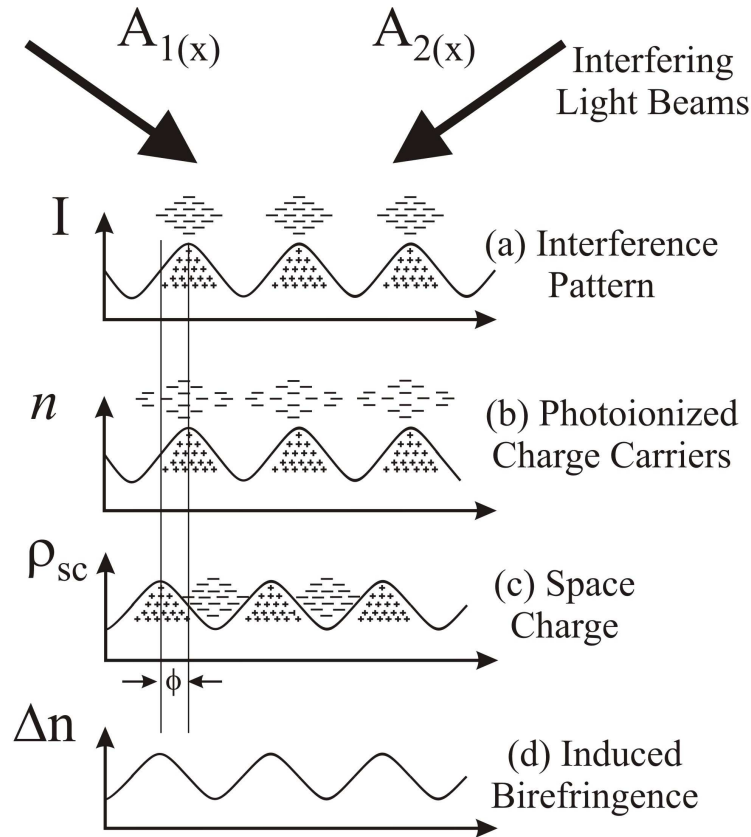


FIGURE 4. A qualitative description of the photorefractive process. (a) Formation of the interference pattern. (b) Generation of the free charge carriers. (c) The distribution of the trapped space charge. (d) The spatial modulation of the index of refraction (birefringence).

The electric field induced by the space charge induces a modulation in the index of refraction through the electrooptic effect. In crystals at the ferroelectric phase the electrooptic effect is linear. Therefore, the modulation of the index is spatially correlated with the space charge field, and hence with the interference pattern of the excited illumination (Figure 4d). (The PR effect was discussed at length in several monographs and papers. cf. references 7, 8, 9 and 10).

In crystals at the *paraelectric* (PE) phase the electrooptic effect is *quadratic* and hence the induced change in the index of refraction is given by

$$\Delta n = (1/2) n_o^3 g_{\text{eff}} P^2 \quad [8]$$

where Δn is the induced birefringence, n_o is the refractive index, g_{eff} is the effective quadratic electrooptic coefficient, and P is the dc (or low frequency) induced polarization (REF11).

(Note that equation [8] that is generally a tensorial equation is brought here in its scalar form with the appropriate *effective* quadratic electrooptic coefficient (REF11)).

Consider the case of a transmission sinusoidal grating (Figure 2). The grating is formed by the interference of two plane waves with wave vectors \mathbf{k}_1 and \mathbf{k}_2 respectively ($|\mathbf{k}_1|=|\mathbf{k}_2|=k$), incident symmetrically with respect to the normal to the crystal surface. The light intensity of the interfering beams during the writing of the hologram is given by $I=I_0+I_1\cos(\mathbf{K}\cdot\mathbf{r})$, where \mathbf{K} is given by $\mathbf{K}=\mathbf{k}_1-\mathbf{k}_2$. During the PR process this interference pattern generates a space charge given approximately by $E_{sc}(\mathbf{r})=E_{sc}\cos(\mathbf{K}\cdot\mathbf{r}+\phi)$. If an external electric field E_R is applied to the crystal, then the electric field in the crystal is given by

$$\mathbf{E} = E_R + E_{sc}(\mathbf{r}) \quad [9]$$

At the PE phase the induced polarization \mathbf{P} is in the linear region, namely:

$$\mathbf{P} = \epsilon_0 (\epsilon_r - 1) \mathbf{E} \approx \epsilon_0 \epsilon_r \mathbf{E} \quad [10]$$

where ϵ_0 is the dielectric permittivity, ϵ_r is the relative dc dielectric constant, and it is assumed that the crystal is slightly above T_c so that $\epsilon_r \gg 1$. Since the electrooptic effect is quadratic the induced birefringence is given by

$$\begin{aligned} \Delta n &= (1/2) n_0^3 g_{eff} \epsilon_0^2 \epsilon_r^2 [E_R + E_{sc}(\mathbf{r})]^2 = \dots \\ \dots &= (1/2) n_0^3 g_{eff} \epsilon_0^2 \epsilon_r^2 [E_R^2 + 2E_R E_{sc}(\mathbf{r}) + E_{sc}^2(\mathbf{r})] \end{aligned} \quad [11]$$

Thus the induced birefringence will contain three terms: (i) a constant shift proportional to $(E_R)^2$; (ii) a linear grating proportional to $E_{sc}(\mathbf{r})$; and (iii) a quadratic grating proportional to $[E_{sc}(\mathbf{r})]^2$.

The effect of the induced birefringence given by [11] on an incoming light beam with wavelength λ_R , entering the crystal with an internal angle of incidence θ_B , which fulfills the Bragg condition [2] for a grating with period $\Lambda=2\pi/K$ is as follows: The term proportional to $(E_R)^2$ does not contain spatial information but introduces a constant shift to the index of refraction. This term may cause a violation of the Bragg condition. However, if the incoming beam enters the crystal at an angle θ' (Figure 2), then Snell's law requires that $\sin\theta' = n_0 \sin\theta_B$.

Hence, the Bragg condition is not violated in the transmission configuration and this term does not affect the diffraction. The term proportional to $[E_{sc}(\mathbf{r})]^2$ is a quadratic grating for which the grating vector is $2K$. Hence, the quadratic grating does not contribute to the diffraction of the incoming beam since the Bragg condition is not fulfilled. The term proportional to $E_o E_{sc}(\mathbf{r})$ induces a grating for which the incoming beam fulfills the Bragg condition. The amplitude of this grating $\delta(\Delta n)$ is given by

$$\delta(\Delta n) = n_0^3 g_{\text{eff}} \epsilon_o^2 \epsilon_r^2 E_R E_{sc}(\mathbf{r}) \quad [12]$$

This grating will cause diffraction of the incoming beam with a diffraction efficiency given by [3]. Thus, the power of the switched beam will be given by

$$P_{\text{diff.}} = P_{\text{in}} e^{-\alpha d} \sin^2 \left(\frac{\pi n_0^3 g_{\text{eff}} \epsilon_o^2 \epsilon_r^2 E_R E_{sc}(\mathbf{r}) d}{\lambda_R \cos \theta} \right) \quad [13]$$

where P_{in} is the power of the incoming beam, α is the absorption coefficient of the crystal, and d is the crystal thickness.

In summary, the information carrying space charge field is transformed into a modulation of the refractive index only in the presence of an external electric field. Therefore, the use of the quadratic electrooptic effect enables an analog control of the efficiency of the reconstruction of the information. This phenomenon is known as the voltage controlled PR effect (REF12).

It should be noted that the effect of also electric fields on PR gratings was investigated in ferroelectrics such as SBN, where the effect of the applied field on the diffraction is achieved by the Bragg detuning mechanism (REF13).

3.2. The Voltage Controlled Photorefractive Effect in KLTN

The implementation of EH based devices (EHD) necessitated the development of a special photorefractive crystal: potassium lithium tantalate niobate (REF14) (KLTN). As pointed out above the optimal work point for the EHD is above the Curie point where the Curie-Weiss law holds and the induced polarization is given by [10]. At the same time it is

desirable to approach the Curie point as much as possible so that $\epsilon_r \approx 10^4$ and large polarizations can be induced with moderate fields.

The first demonstration of the voltage controlled PR effect was done in potassium tantalate niobate (KTN) doped with copper and vanadium (REF12). KTN is a ferroelectric oxide in which large photorefractive effects were demonstrated. The Curie temperature T_c of KTN is determined by the ratio Nb/Ta at the rate of $\Delta T_c \approx 8.5\%$ per mole of Nb in the crystal (REF15). Thus, controlling this ratio during the growth of the crystal enables setting the work point to the desirable range. In KTN crystals in which the concentration of Nb exceeds 30% per mole, the optical quality is substantially deteriorated in the proximity of the phase transition. Therefore, KTN is not the optimal medium for devices in which the desirable work point is approximately at room temperature. This limitation was obviated in KLTN that is a derivative of KTN (REF16, 17). It was found that the addition of Li to $\text{KTa}_{1-x}\text{Nb}_x\text{O}_3$ (KTN) causes an increase in the ferroelectric phase transition temperature T_c , while maintaining high optical quality in the temperature region close to the transition. It was found that KLTN doped with copper is particularly suitable for the implementation of EHDs. The PR process in this material is produced by photoexcitation of electrons from Cu^+ ions by photons with energy exceeding 2 eV that are transported and eventually trapped by Cu^{++} ions.

High quality KLTN crystals were grown using the Top Seeded Solution Growth (TSSG) Method (REF18). By adjusting the Nb/Ta and Li/K ratios in the flux it was possible to set T_c in the range between 100K to 400K while maintaining high optical quality in the region close to the transition.

In particular, KLTN crystals doped with copper and vanadium were grown with $T_c \approx 290\text{K}$, in which the optical quality in the region slightly above T_c (i.e. in the region $T \geq T_c + 4\text{K}$) was especially good.

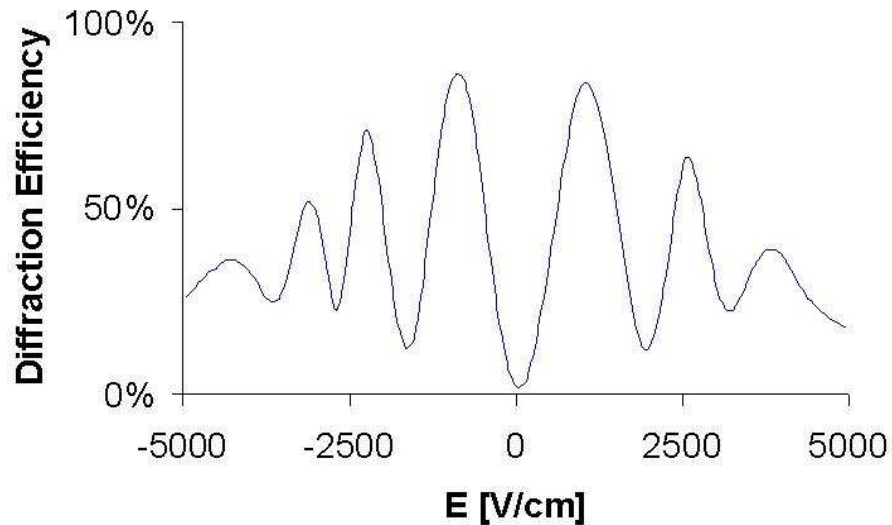


FIGURE 5. Experimental results of the diffraction efficiency vs. the electric field of a Bragg grating in the transmission symmetrical configuration in KLTN.

Typical measurement of the diffraction efficiency of a symmetrical transmission grating (Figure 2) as function of the electric field is given in Figure 5 (REF19). The crystal was potassium lithium tantalate niobate (KLTN) doped with copper and vanadium with $T_c = 18.5^\circ\text{C}$. A sample of $1.5 \times 1.5 \times 2 \text{ mm}^3$ was cut along the crystallographic axes. Gold electrodes were deposited orthogonal to the optical axis. The grating was written at 532 nm with intensity of approximately 10 mW per writing beam. The exposure time was 15 seconds. The grating was written and read at $T = 25^\circ\text{C}$.

Note that in a symmetrical transmission grating the Bragg condition is compensated by the Snell refraction at the entrance plane. Therefore the diffraction efficiency is expected to follow [13]. However, as can be seen in Figure 5 the dependence of η_{diff} on the applied field deviates from [13] as the strength of the applied field increases. This is due primarily to the saturation of the induced polarization that occurs in the vicinity of the phase transition (REF20).

3.3 Assessment of the KLTN crystal as Electroholographic Medium

In order to assess the performance limits of the KLTN based EHDs it is necessary to analyze the behavior of the KLTN crystal as a holographic storage medium. The latter is manifested by several parameters that will henceforth be considered.

The Holographic Storage Capacity

The material property that limits the storage capacity in a holographic system is the maximum induced change in the refractive index that can be generated in the holographic storage medium. One of the critical parameters that govern the performance envelope an EHD is the maximum diffraction efficiency of the grating. In a die of given dimensions, the latter is also limited by the maximum induced change in the refractive index that can be generated by the EH process. Therefore, the holographic storage capacity is a useful parameter for comparing the potential performance of EH media. Mok et. al. (REF21) suggested to characterize the storage capacity of a holographic system by the figure of merit $M/\#$ defined as

$$M/\# = M\sqrt{\langle\eta\rangle} \quad [14]$$

where $\langle\eta\rangle$ is the average diffraction efficiency of the stored holograms. It is shown that for $M \gg 1$ the $M/\#$ is independent of M , it does however depend on the angular and wavelength configuration of the reading system. Detailed measurements of the $M/\#$ of KLTN are described and discussed in Reference 22. The $M/\#$ of copper and vanadium doped KLTN in the configuration of an EHD, where the reading wavelength is in the range of the WDM wavelengths (approximately $1550\text{nm} \pm 100\text{nm}$), and the (external) angle between the input beam and the switched beam is 90° , were performed recently by M. Puterkovsky (REF23). $M/\#=2.13$ was obtained in a 1.65 mm thick sample, operating at $T_c+5^\circ\text{C}$ under applied field of 3.6 kV/cm. This result is equivalent to $M/\#\approx 20$ in the same sample operating under the same conditions with a readout wavelength of 500 nm. Note that this result is exceptionally high compared to previous results obtained in both LiNbO_3 and KLTN as reported in references 21 and 22 respectively.

The Photorefractive Sensitivity

The light energy required to generate the space charge grating during the fabrication process of the EHD is governed by the PR sensitivity S . S is defined as the generated change

in the index of refraction per absorbed light energy in a unit volume of the material. In terms of S , the dependence of the change in the refractive index generated by the PR process on the exposure time τ , and the intensity of the writing beams I_0 is given by

$$S = \frac{\delta(\Delta n)}{I_w \alpha_w \tau} \quad [15]$$

where α_w is the absorption of the EH medium at the writing wavelength. The PR sensitivity in copper and vanadium doped KLTN was measured recently by M. Puterkovsky (REF23). It was found that at the wavelengths range around $\lambda \approx 500\text{nm}$ $S \approx 1.3 \cdot 10^{-4} \text{ cm}^3/\text{J}$. Thus, in order to generate a grating with amplitude of $\delta(\Delta n) = 10^{-4}$ in an EH medium with $\alpha_w = 1 \text{ cm}^{-1}$, it is required to use $I_w = 1 \text{ W}$ for approximately 1 seconds.

Holograms stability

The sustained stability of electroholograms over long periods of time under the operating conditions is essential for the establishment of Electroholography as a viable technology. The stability of electroholograms implemented by the PR process is determined by the stability of the space charge that forms the electroholograms in their latent state. In principle, if free charge carriers are generated in the EH medium they will tend to restore thermodynamic equilibrium by migrating under the influence of the space charge field in a direction that causes the erasure of the space charge. Two mechanisms may cause the generation of charge carries in the electroholographic medium: optical excitation and thermal excitation. Both mechanisms may lead to the decay of the latent electroholograms and therefore it is imperative to quantify their effect.

Optically induced decay of the holograms: Electroholograms produced by the PR process are by definition subject to erasure during readout (REF24). Recall that in its latent form the EH grating is a space charge grating formed by the excitation of trapped charge carriers that are transported and retrapped. Illuminating a PR grating will excite charge carriers that will drift by the influence of the space charge field, and will cause the decay of the latter. Thus, illumination at a wavelength at which the PR sensitivity is zero will not cause erasure during readout since the illuminating photons do not possess enough energy to excite the charge carriers. It is therefore required that at the operating wavelengths the PR sensitivity of the PR medium used in the device will be zero. It is further required that the PR medium in the EHD

will not be exposed to stray light after the writing of the grating except for the lightwave emanating from the fiber.

In KLTN crystals doped with copper the PR process is produced by redistribution of electrons between Cu^+ and Cu^{++} ions. The energy required to photoionize Cu^+ ions exceeds 2eV. Hence, it is not expected that the photons at the operating wavelength ($h\nu \geq 1.25 \mu\text{m}$) will have sufficient energy to cause photoexcitation of electrons from the Cu^+ ions.

Measurements of the absorption and photoconductivity in copper doped KLTN indicate that the PR sensitivity at the wavelengths range of the DWDM bands is indeed zero. Therefore, optical erasure of the gratings is not expected to happen in this wavelengths range.

Thermal decay of electroholograms: Thermally excited charge carriers are expected to cause erasure over time of the space charge that forms the electrohologram. We distinguish between two possible mechanisms of thermal excitation: The intrinsic mechanism, and the extrinsic mechanism. The intrinsic mechanism, relates to the thermal excitations of the charge carriers that form the PR space charge. In copper doped KLTN two intrinsic thermal decay processes are possible: In the first an electron is thermally excited from a Cu^+ state, drifts under the space charge field, and is eventually captured by a Cu^{++} state. The second process is the thermal release of a hole from a Cu^{++} state to the valance band, and its subsequent capture in a Cu^+ state. The probability for a thermal emission of a charge carrier is given by $\nu_0 \cdot \exp(-E_a/k_B T)$, where ν_0 is the 'attempt to escape' frequency, and E_a is the energy barrier that needs to be surmounted. In KLTN, a Cu^+ level is located more than 2 eV below the conduction band edge, and the Cu^{++} states are located a similar energetic distance away from the valance band edge. Even for an over estimation of the 'attempt to escape frequency' (10^{20} Hz) the time scale of thermal release of carriers is over 1000 years. Hence, erasure of the electrohologram due to intrinsic thermal decay of the space charge can be discarded.

The second mechanism is the extrinsic mechanism. The PR medium may contain localized states other than those that carry the PR space charge. These states can reside close to the band gap edges of the material so that their activation energy is substantially less than that of the PR states. Thermal excitation of charge carriers from such states will cause the decay of the space charge forming the latent electrohologram, and hence the erasure of the latter.

The extrinsic mechanism can be obviated by removing the extrinsic states either during the crystal growth or by some treatment after the growth.

The lifetime of the electroholograms is defined as the time the diffraction efficiency is reduced to 90% of its original value under the operating conditions. Very long lifetimes are

measured through the acceleration of the thermal relaxation processes by controlled heating of the electroholograms. Using this method, it was found that in copper doped KLTN, electroholograms that were subjected to the process the removes the extrinsic states have lifetimes of over ten years.

4. The Basic Electroholographic Switch Module

4.1 The Architecture and Functionality Basic EH based Switch Module

The basic EH based switch *module* (EHSM) is an array of single EHDs. The basic single EH based *device* is an ECBG tuned to a single wavelength on the ITU grid as presented schematically in Figure 6. The input signal is incident onto the grating after it was collimated by the input collimator. The period of the grating is chosen so that the diffracted beam emerges out of the device at 90° to the input beam.

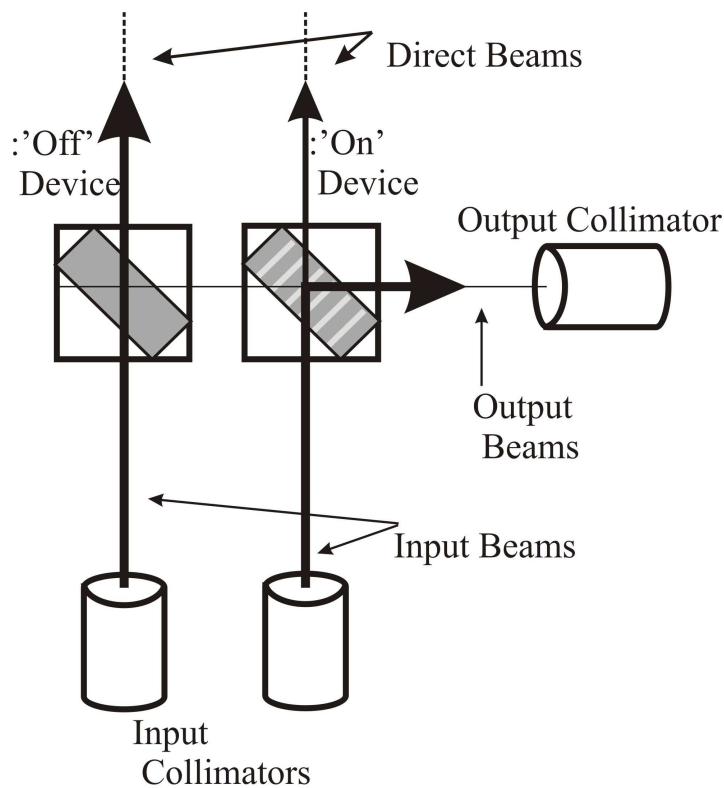


FIGURE 6. The basic Electroholography based device in the latent and active states.

Consider the operation of the device when the input signal contains one component (wavelength) of the DWDM signal. When the ECBG is in the 'off' state the input beam propagates unaffected through the device. When the ECBG is in the 'on' state (the electric field is applied) the input beam is diffracted and emerges out of the device and collected by

the output collimator. As the efficiency of the diffraction is not 100%, a residue of the input beam emerges directly out of the device and continues along the input optical axis.

In the basic EH based switch *module* the EHDs are arranged in a ‘Full Crossbar’ configuration in which the columns are inputs and the rows are outputs. Each column in the cross bar is allocated a wavelength on the ITU grid. Namely, the EHDs that constitute the column are tuned to the same wavelength. The output (diffracted) beams that propagate along the optical axis of a row are coupled by one output collimator into an output fiber. The input WDM signal entering the device through the input port is first demultiplexed into its single (one wavelength) components. Each of these components is then collimated and directed along the optical axis of its respective column. By activating one of the EHDs the respective component will be diverted to the selected output. An EHSM constructed of five input columns and three output rows is presented schematically in Figure 7. The various functions implemented by the EHSM are demonstrated in Figure 7.

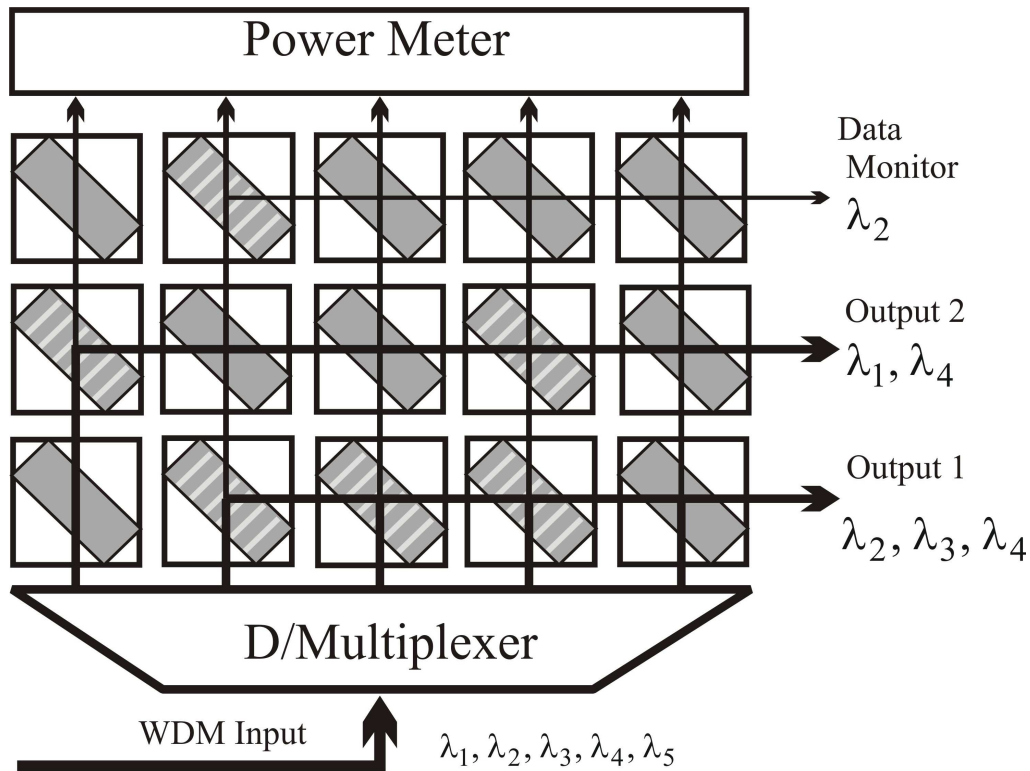


FIGURE 7. An electroholographic switch module performing grouping, multicasting, power management, and data monitoring.

Grouping: The EHSM can regroup the input WDM channels into subgroups, and assign each subgroup to an output port. (In Figure 7: the group $\{\lambda_2, \lambda_3, \lambda_4\}$ is assigned to output 1, and group $\{\lambda_1, \lambda_4\}$ is assigned to output 2). Note that the ‘grouping’ function is in fact an extension of the basic ‘dynamic drop’ function that describes the switching of one single wavelength channel to an output port. It can also be used to perform the ‘add’ function as illustrated schematically in Figure 8. The ‘add’ WDM channels are directed along the input row and are selected by the EHD of the respective output row. (In Figure 8, $\{\lambda_1, \lambda_2, \lambda_4, \lambda_5\}$ are carried by the input, $\{\lambda_2, \lambda_5\}$ are directed to output 1 and $\{\lambda_1, \lambda_4\}$ are directed to output 2).

Multicasting: The EHSM can multicast the power of each of the input single wavelength channels between several outputs. Multicasting is accomplished by controlling the level of the applied electric field that governs the diffraction efficiency of the EHDs. (In Figure 7: $\{\lambda_4\}$ is distributed between outputs 1 and 2).

Power management: The EHSM enables the management the power of the single wavelength channels in each of the subgroups. Power management is accomplished in three steps: (i) Monitoring the residual power that continues through the column along the input optical axis; (ii) estimating the switched power by assuming that the efficiency of the switching operation is known, and (iii) governing the switching efficiency by controlling the level of the applied electric field.

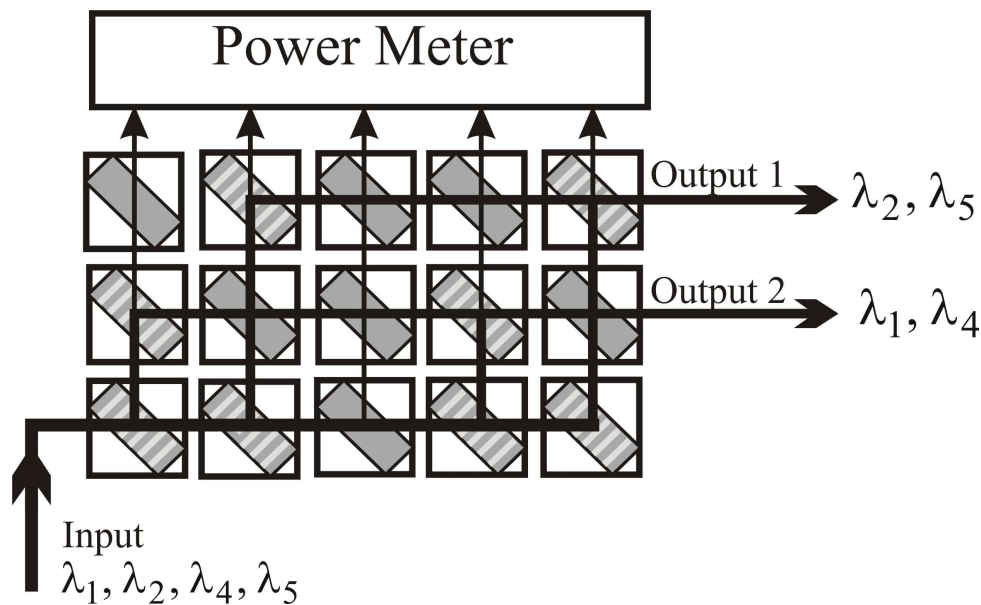


FIGURE 8. An electroholographic switch module performing the ‘Add’ operation.

Data Monitoring: The EHSM enables monitoring the data of the single wavelength channels without interfering with the switching operation. In principle, data monitoring can be accomplished by sampling the residual power that continues through the column along the input optical axis. This, however, would require the placement of a dedicated receiver at the top of each column. If continuous monitoring of all the channels in parallel is not required, sparse sampling can be accomplished by the ‘data monitoring’ row that diverts the selected channel to one receiver. (In Figure 7, $\{\lambda_2\}$ is diverted to the data monitor).

4.2 The Performance parameters of the Basic EH Switch Module.

The basic building block of EH based systems are the generic EHDs. The latter are grouped together to form EHSMs of different architectures according to the specific application of the EH based system. In order to assess the performance envelope of EH based systems it is necessary to evaluate the primitive performance parameters of the generic EHDs.

Operating wavelengths range: The EHD can be operated at wavelengths that do not affect the PR grating. Namely, the photons of the operating wavelengths do not have enough energy to photo-ionize charge carriers that can erase the grating. In KLTN crystals in which the PR impurity is copper this implies $\lambda > 1.25 \mu\text{m}$. It is also required that the operating wavelengths are not absorbed in the crystal. In copper doped KLTN the latter requirement implies $\lambda < 1.7 \mu\text{m}$.

Data throughput rate: In principle, the data throughput carried by light beams that propagate through an EHD is not affected by the diffraction that occurs in an active switch, provided the light is linearly polarized along a principal axis of the switch. In reality the polarization of the lightwave that emerges from the fiber is not linearly polarized and varies over time. The bit error rate at very high data throughput rates will therefore be affected by the polarization mode dispersion and polarization dispersion loss that occurs in the switch.

Insertion Loss: Consider the path along which the lightwave propagates through an EHSM (Figures 6, 7 and 8). The light propagating in the input fiber enters the module from the input collimator as a collimated beam. It then propagates through a series of passive EHDs along the input column until it reaches the active switch where it is diffracted along the output row. It then propagates through passive switches until it is collected by the output collimator and coupled into the output fiber. The insertion loss in the EHSM is given by

$$IL = IL_{\text{Collimators}} + N_{\text{ps}} IL_{\text{ps}} + IL_{\text{as}} \quad [15]$$

where:

- $IL_{\text{collimators}}$ is the insertion loss due to the coupling between the input and output collimators. $IL_{\text{collimators}}$ takes into account the divergence of the beam in the module and is therefore affected by the length of the path traversed by the beam. $IL_{\text{collimators}}$ also depends on the alignment procedure of the collimators. For example, a beam with diameter of 0.6 mm traversing through a path length of 7 cm, and collimated so that the waist of the beam is in midway between the collimator will cause insertion loss of 1.5 dB.
- IL_{ps} is the insertion losses in one EHD at the passive mode. The bulk KLTN crystal does not absorb light at the operating wavelengths. Therefore, IL_{ps} is determined primarily by the loss of reflection, scattering, and absorption at the input and output surfaces of the switch. It is also affected by the accuracy of the die parallelism achieved in the processing. It is expected that high quality polishing and antireflection coating procedures will result in $IL_{\text{ps}} = 0.3\%$.
- N_{ps} the number of passive switches the beam passes through. Note that N_{ps} depends on the specific route of the beam in the module. Consider for example the 5x2 module illustrated in Figure 7. The data channel at λ_1 that is switched to output 2 goes through the longest route ($N_{\text{ps}}=5$), whereas the data channel at λ_5 that is switched to output 1 goes through the shortest route ($N_{\text{ps}}=0$).
- IL_{as} is the insertion loss in the active switch given by

$$IL_{\text{as}} = IL_{\text{ps}} + 10 \log_{10}(1 - \eta_{\text{diff}}) \quad [16]$$

where η_{diff} is the diffraction efficiency in the active switch.

Polarization Dependence: The state of polarization of the lightwave signal emerging from the fiber into the switch is different from the one entering the fiber at the transmitter side and varies with time according to various environmental conditions such as temperature and stress. Thus, the state of polarization of the lightwave entering the switch fluctuates with time constants ranging from subseconds to hours according to the extent and rate of change of the said environmental conditions (REF25). In order to avoid loss of data it is required that the

switching operation will not depend on the state of polarization of the incoming lightwave signal.

The effects of variations in the state of polarization of the propagating signal are quantified by the polarization dependent loss (PDL), and the polarization mode dispersion (PMD). The PDL quantifies the loss of power of the switched lightwave signal as function of its state of polarization. The PMD quantifies the time delay between pulses that are launched into the switch with orthogonal states of polarizations.

A switching operation that is implemented in a crystal by diffraction from a photorefractive grating is in principle polarization dependent. This is due to the fact that the electrooptic tensor that governs the diffraction efficiency is by definition polarization dependent (REF11). Minimization of the PDL and PMD can be achieved at the device level by polarization independent configuration of the EHD, and at the module architecture level by polarization diversity.

Polarization independent configuration of the switch is accomplished by exploiting the symmetry relations between the elements of the electrooptic tensor of the EH medium. This is done by selecting the direction of propagation of the lightwave, the grating vector, and the applied field with respect to the crystal principle axes so that the diffraction efficiency will be independent of the state of polarization.

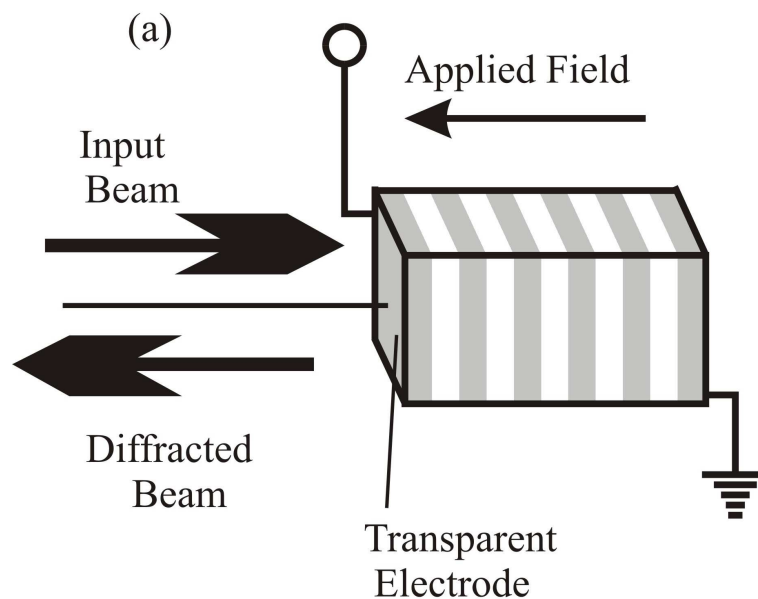


FIGURE 9. An Electroholography based switch device in the reflection configuration in which is PDL and PMD free.

As an example consider the EHD with reflective configuration illustrated in Figure 9. Here the optical axis of the switch coincides with a principle axis of the KLTN crystal and the grating vector of the EH grating. Applying the electrical field along the optical axis causes the optical axis to become the axis of symmetry of a uniaxial crystal. Thus, an input beam propagating along the optical axis will be diffracted in the opposite direction with diffraction efficiency independent of its state of polarization. Note that in the reflective configuration the Bragg detuning is not compensated by the Snell refraction at the crystal input plane. Therefore, the diffracted efficiency is given by [5].

In polarization diversity schemes the two orthogonal states of polarization of the incoming lightwave signal are switched separately and then reunited. Thus the single EHD in an EHSM consists of two crystals each switches one polarization branch of the same single wavelength channel of the WDM lightwave signal.

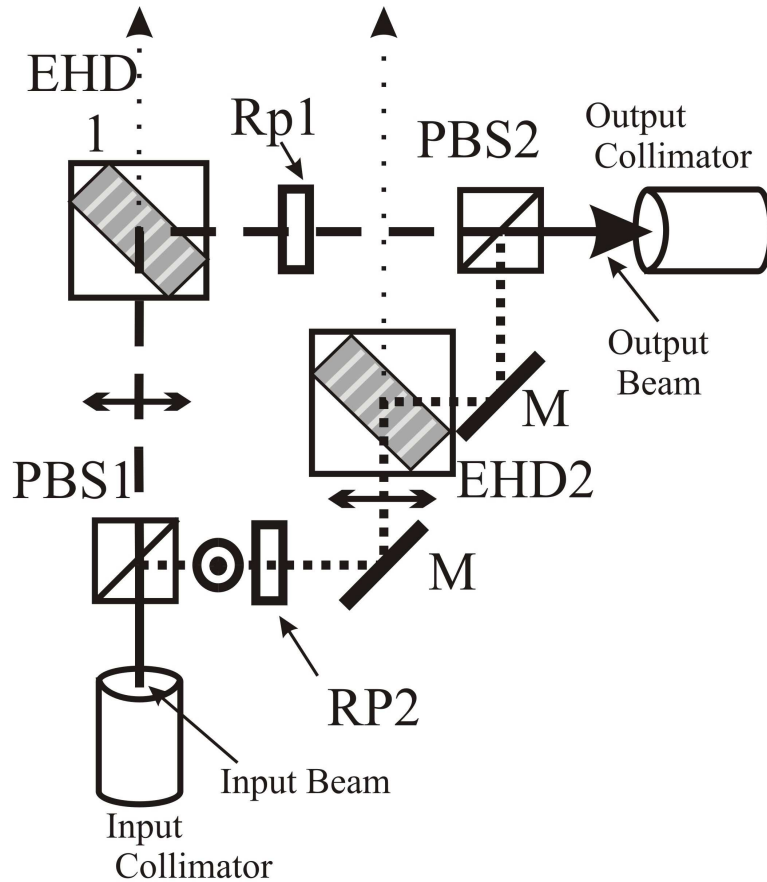


FIGURE 10. An element of the electroholographic switch module in which an implementation of the polarization diversity architecture is demonstrated.

Consider Figure 10 demonstrating an optional implementation of polarization diversity in one route of the EHSM. The polarizing beam splitter PBS1 at the input separates the incoming

collimated lightwave signal into its two orthogonal states of polarization. Assume that maximum efficiency is achieved when the polarization of the lightwave signal is in the plane of the device. Branch 1 (the dashed line in Figure 10) is switched by switching device EHD1 and then its polarization is rotated by 90° by the $\lambda/2$ retardation plate RP1. The polarization of Branch 2 (the dotted line in Figure 10) is first rotated by RP2 to the plane of the device and then switched by EHD2. The two branches are then united in the polarizing beam splitter PBS2. Thus both branches are switched with maximum efficiency. Note that the path length of both branches is the same. Preliminary measurements of the PDL vs. the wavelength were measured in a EHSM similar to the one illustrated in Figure 10. The grating was written to operate at $\lambda_0=1550\text{nm}$. It was found that $\text{PDL}(\lambda_0) < 0.07 \text{ dB}$ and $\text{PDL}(\lambda \pm 0.5 \text{ nm}) < 0.4 \text{ dB}$. In general it found that

$$\frac{d}{d\lambda} \text{PDL}(\lambda) \approx 0.75 \text{ dB/nm} \quad [17]$$

The PMD was also measured in this module and was found to be approximately 0.07 Pico seconds at data throughput rate of 10Gb/sec. The low PMD in this module is also manifested in a bit error rate tests. A lightwave signal at data throughput rate of 40Gb/sec incident into the module with power of 8dBm that yielded $\text{BER} < 2 \cdot 10^{-13}$.

It should be noted that in an EHSM in which polarization diversity is applied it is possible to perform polarization management. The two polarization branches of each single wavelength channel of the lightwave WDM signal can be monitored separately by the direct beams propagating through the two crystals that in this case constitute the EHD. Combining this feature with the fact that the power of the switched (output) lightwave signal is governed by the applied electric field enables intelligent control of each of the polarization components of the signal. This feature may become useful in systems where correction of the polarization of the lightwave signal in real time is required.

Selectivity: The EHD is optimized to function as the basic building block in wavelength selective switching systems. Therefore, the spectral response of the EHD is of paramount importance to the performance envelope of any EH based system. The single switching EHD is in essence an electrically controlled filter. The spectral response of the EHD is derived from the effect of deviating from the Bragg condition [2].

Consider an EHD implemented by an electrically controlled sinusoidal Bragg grating. The maximum switching efficiency of the EHD is obtained when the incident beam fulfills the Bragg condition [2]. When the Bragg condition is not fulfilled the diffraction efficiency will diminish. The level of deviation from the Bragg condition is given by the Bragg detuning factor ξ . If the wavelength of the incident beam is shifted by $\delta\lambda$, ξ will be given by

$$\xi = \frac{\pi}{\Lambda} \cdot \frac{\delta\lambda d}{n \Lambda \cos \theta_B} \quad [18]$$

assuming all other parameters remain fixed. In terms of ξ the diffraction efficiency diminishes according to expression [5]. Deviation from the Bragg condition will also cause the diffracted (output) beam to divert from its original direction ($-\theta_B$) by

$$\delta\theta_{\text{out}} = \frac{\delta\lambda}{2 n \Lambda \cos \theta_B}. \quad [19]$$

The spectral response of the EHD results from the combined effect of the loss of diffraction efficiency and the diversion of the output beam from its original direction. Consider the configuration of the EHD presented schematically in Figure 6. The output collimator is aligned in a fixed position along the Bragg angle of the output beam. Diversion of the output beam from the Bragg angle as a result of shift in the wavelength will reduce the power that is collected by the output collimator.

The combined effect of the loss of diffraction efficiency and the diversion of the output beam from the Bragg angle on the spectral response of an EHD is demonstrated in Figure 11. A grating of thickness $d=1.5\text{mm}$, with period of $\Lambda=1.1\mu\text{m}$ was stored in a KLTN crystal ($n_o=2.3$). The Bragg condition is fulfilled for an input Gaussian beam at $\lambda=1.55\mu\text{m}$ with diameter of 0.510 mm incident at 45° to the plane of incidence of the crystal. The solid line in Figure 11 presents the power diffracted from the crystal and detected by a wide area detector as function of $\delta\lambda$, computed by expression [5].

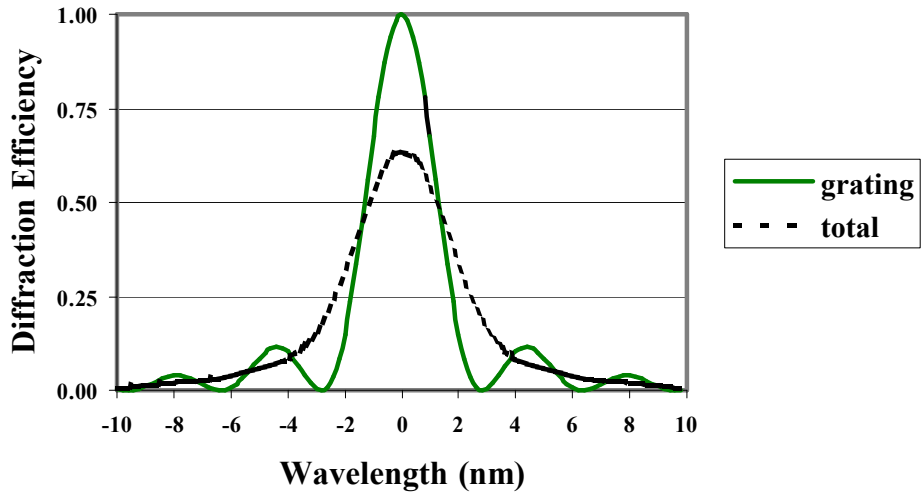


FIGURE 11. The spectral response of an EH based switching device: — The diffraction efficiency of a sinusoidal grating; - - - The output power collected by the output collimator.

The dashed line presents the power collected by a collimator aligned along the Bragg output angle computed by the convolution of the diffraction efficiency expression [5] with the beam profile. Note, that the side lobes arising from the sinc dependence of η on ξ in the pure grating disappear when the output diversion from the Bragg angle $-\theta_B$ is taken into account. It is clear that the spectral bandwidth of the basic EHD presented in Figure 11 cannot support dense WDM applications.

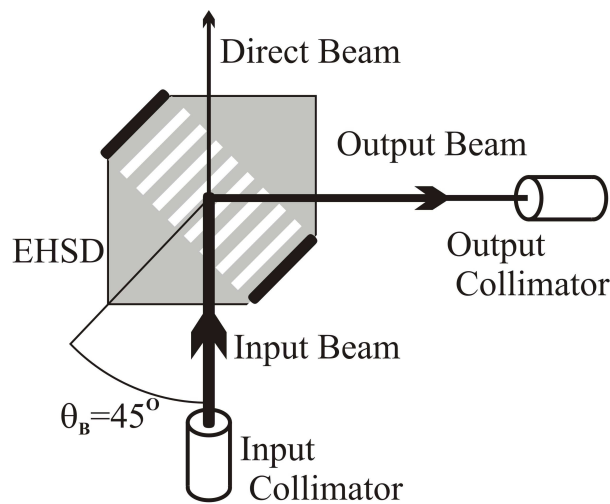


FIGURE 12. An EH based switching device in the 0-90° configuration.

One approach for narrowing the bandwidth is to enlarge the interaction length traveled by the input beam through the grating. This approach will not yield a substantial improvement unless the device size and the beam diameter are enlarged beyond practicality. An alternative approach is to form a grating with a smaller period. The grating period is determined by the Bragg angle and is limited in the simplistic configuration (Figure 6) by the critical angle of the crystal. Note that in the device described above, due to Snell refraction at the plane of incidence of the crystal the Bragg angle is $\theta_B=18^\circ$. This limitation is obviated in the 0-90° configuration presented schematically in Figure 12. Here the angle of incidence into the device is 0° so that Snell refraction does not occur. The grating vector is inclined at 45° to the plane of incidence so that $\theta_B=45^\circ$. The spectral response of an EHD built in the 0-90° configuration is presented in Figure 13.

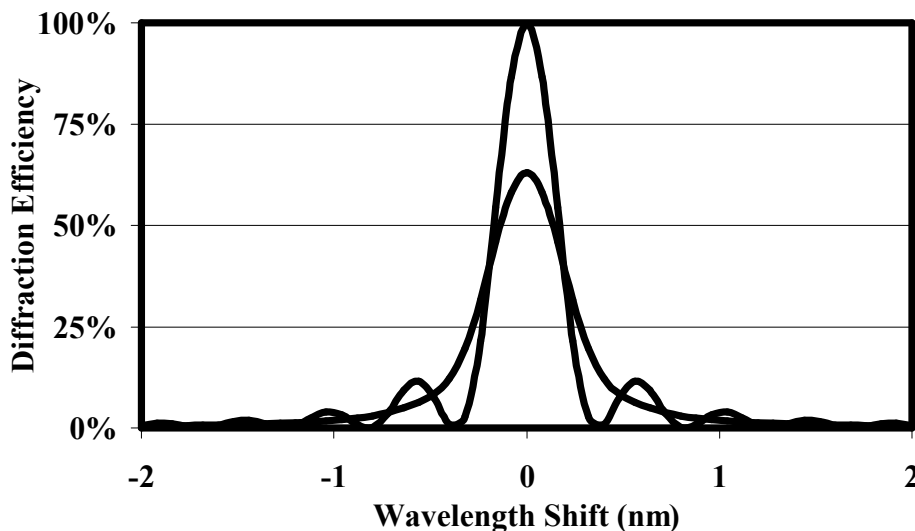


FIGURE 13. The spectral response of an EH based switching device in the 0-90° configuration

The grating period is $0.5 \mu\text{m}$ and the beam diameter is 2mm. Note that this configuration substantially improves the selectivity. Using this configuration selectivity of 100GHz for DWDM applications is obtainable. It should be emphasized however that there is a trade off between the maximum diffraction efficiency that can be obtained and the selectivity when the grating period is of the order of magnitude of the Debye length in the crystal. Increasing the impurity concentration in the crystal can obviate this trade off.

Switching time: We distinguish between two main methods of switching transmitted information across the network, circuit switching and packet switching (REF25). The switching time requirements on the EHD are derived from the switching method employed by the system in which the devices are embedded. Circuit switching systems implement transparent data pipes in which the communication path is intended for long transmissions such as telephone calls. Consequently, set-up and tear down time of the link, and the response time of the system to evolving situations are long, namely, in the milliseconds range. (e.g. the allowed restoration time in a SONET system is 50 milliseconds). The current performance envelope of circuit switching systems is defined under the assumption that the information traffic in the network is primarily voice telephony. As the network will evolve into being more data oriented the performance envelope will have to be redefined. It is expected that the required switching time of the basic switching component will be in the microseconds range. In packet switching systems the data is transmitted in packets that are routed towards their destination at every node of the network according to the address stored in their header. Consequently, the switching time of the basic switching component in the packet switching arena should be faster than the length of the packet, namely, in the nanoseconds to the submicroseconds range.

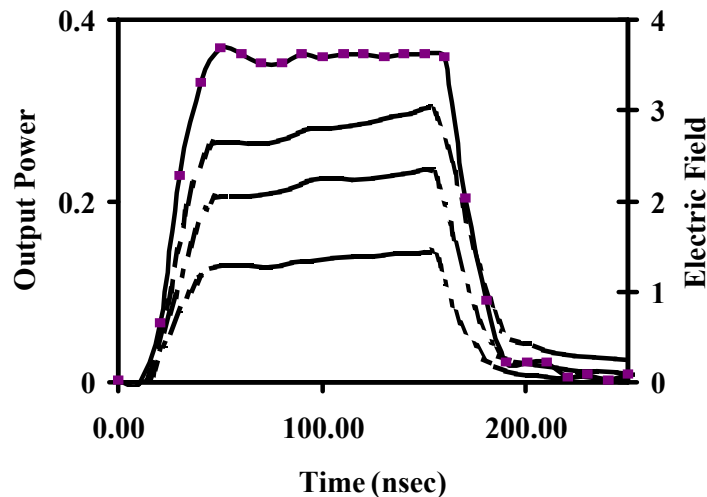


FIGURE 14. The temporal response of an EH based switching device: — The Applied electric field; The diffracted power at: — — $T=T_c+15^\circ\text{C}$; — — — $T=T_c+20^\circ\text{C}$; — .. — $T=T_c+30^\circ\text{C}$

The switching time of the EHD is governed by the physical mechanism of the switching operation. Consider expression [8], [10] and [12] that presents the phenomenology of this

mechanism PR paraelectrics. The application of the electric field to the latent electrohologram causes first to induce a polarization in the medium as given by expression [10]. The induced polarization couples with polarization field induced by the space charge and through the quadratic electrooptic effect causes a change in the index of refraction.

The desired working point of a PR paraelectric EHD implemented in a KLTN crystal is slightly above the Curie temperature. The critical slowing down of the dielectric response in the vicinity of T_c causes the dielectric response (*i.e.* the time the applied field induces the polarization) to be the dominant factor governing the temporal behavior of the switch. The induction of the changes in the index of refraction through the quadratic electrooptic effect is at time scales that are much shorter than the dielectric response of the crystal. Consequently it is expected that the rise time and fall time of the EHD will be in the nanosecond range. Consider Figure 14 in which the spectral response for an EHD is presented. The diffracted power follows the temporal behavior of the driving electric field. The rise time demonstrated in Figure 14 is less than 20 nanoseconds (defined as the time needed for the diffracted light to rise from 10% to 90% of its maximum power). Note that as T_c is approached, the slowing down of the dielectric response becomes apparent causing a trade off between the response time and the diffraction efficiency manifested in the insertion loss of the device. It is expected that the response time of EH based switching will not be shorter than a few nanoseconds. Therefore, EH based switching can become the platform for introducing the WDM technology to the packet/burst switching arena in applications that do not require switching times shorter than a few nanoseconds.

5. Applications of Electroholographic Switching.

The EH based switching device is a generic device, and as such can be the building block in a variety of wavelength selective switching applications implemented by different configurations. We henceforth present two applications that are based on the EH based switching device, an EH based dynamic add drop multiplexer and an EH based cross connect.

5.1 The Electroholographic dynamic optical add drop multiplexer.

The EH based dynamic optical add drop multiplexer (DOADM) is a straightforward application of Electroholography. Consider Figure 15 in which a possible implementation of an EH based DOADM unit is illustrated.

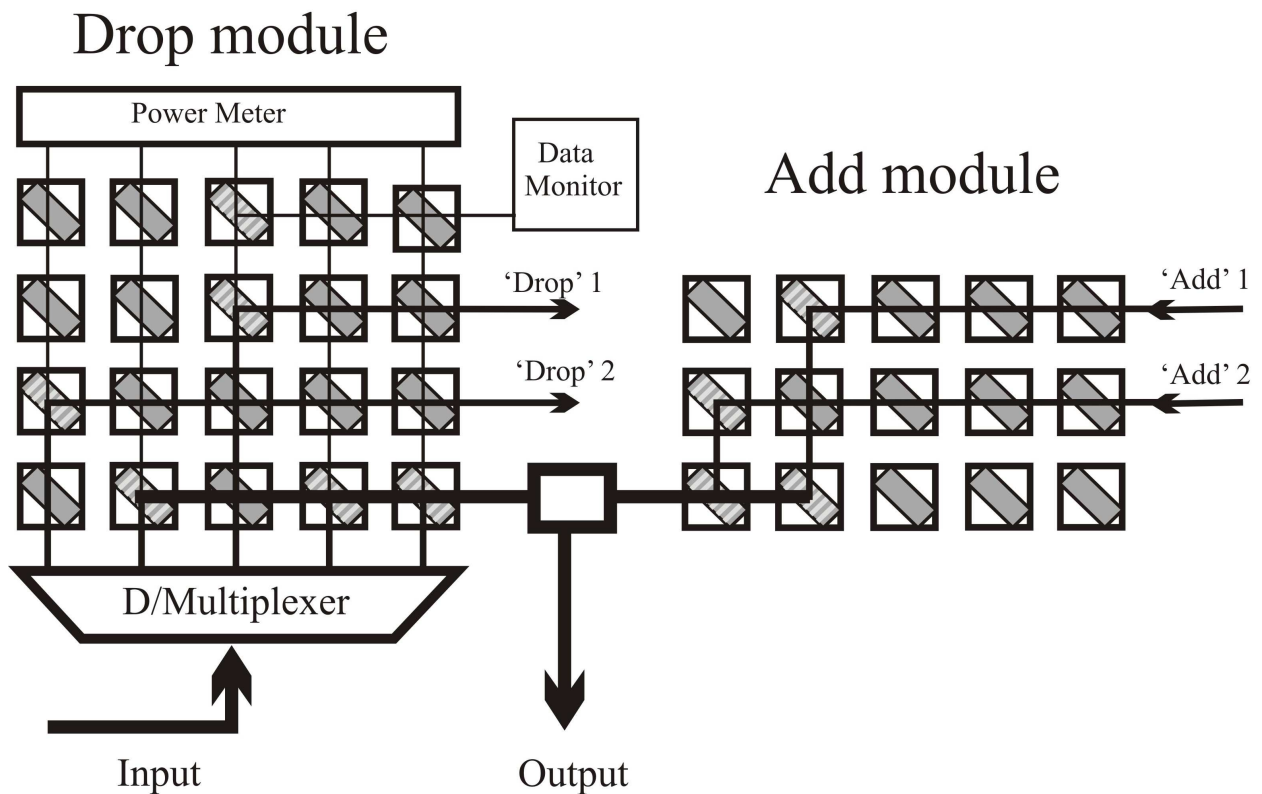


FIGURE 15. Electroholographic dynamic optical add drop multiplexer.

The DOADM in Figure 15 is designed to be installed in a Metro or inter-office ring. The DWDM lightwave entering the unit through the input port is first demultiplexed into the single wavelength channels. The latter are regrouped by the ‘Drop’ module into three groups:

Local ‘drop’ 1, local ‘drop’ 2, and an ‘express channel’ that continues to the output port and onward to the ring. The ‘add’ module contains two ‘add’ ports that are coupled to the output port of the unit. In addition the unit contains power management and data monitoring capability attached to the ‘drop’ module.

The specific configuration of the EH based DOADM illustrated in Figure 15 involves several design choices:

1. In Figure 15 a DWDM demultiplexer is used to break the DWDM lightwave into its single wavelength channels. Alternatively, it can be implemented by a row of EHDs, or in the case of DWDM lightwave with many wavelength channels by a series of interleavers interlacing a series of EH based ‘drop’ modules.
2. The number of ‘add’ and ‘drop’ channels implemented in the unit illustrated in Figure 15 is arbitrary and is application dependent. Moreover, in most applications, each local ‘add’ port and each local ‘drop’ port is required to handle one wavelength channel.
3. The incorporation of optical amplifier in the EH based DOADM is simple since the unit has power management capabilities.

5.2 The Electroholographic cross connect.

The EH based cross connect fully exploits the potential of Electroholography as a wavelength selective switching technology. As such the EH based cross connect falls into the system category of “Intelligent Optical Switches” (IOS). The IOS are expected to integrate the isolated DWDM point-to-point links into a truly optical network that is operated in an intelligent and integrated fashion. More specifically the expected benefits of the IOS are improved bandwidth efficiency and scalability, faster provisioning speed, and significant cost, power and footprint savings.

A basic cross connect unit based on EH is illustrated in Figure 16. The unit in Figure 16 is capable of interconnecting four DWDM lightwaves each carrying N single wavelength channels. Accordingly, the unit is built of four EHSM each of which has N wavelength columns, four output rows, a management row, and a power management unit. The respective output rows of the EHSMs are coupled to form the respective output port of the cross connect. The lightwave emanating from each input fiber is first demultiplexed into its single wavelength channels, which are then regrouped by the EHSM assigned to this fiber according to their respective destinations. Finally, the four subgroups that are allocated to the same output fiber are coupled together and are transmitted out of the respective output port. Note, that each EHSM is equipped with both power management and data monitoring capabilities that are integrated with the cross connect operation.

The $4 \times N \times 4$ architecture illustrated in Figure 16 demonstrates the underlying principle of operation of the EH based cross connect in its most simplistic form. It does not extract the full potential of EH based wavelength selective switching for implementing optical cross connect architectures. Other design options are possible:

1. The dimensions of the cross connect, namely, the number of single wavelength channels per fiber, the number of input ports, and the number of output ports is application dependent.
2. The architecture presented in Figure 16 is transparent. The single wavelength DWDM channels propagate through the unit unaffected assuming that data regeneration is not necessary. (Note that the latter is inherently electronic). The EH based cross connect enables the integration of transparent and opaque switching in the same unit on a cost effective basis. This is accomplished by assigning an input fiber and an output fiber to the task. The output fiber is connected to the input of an OEO unit.

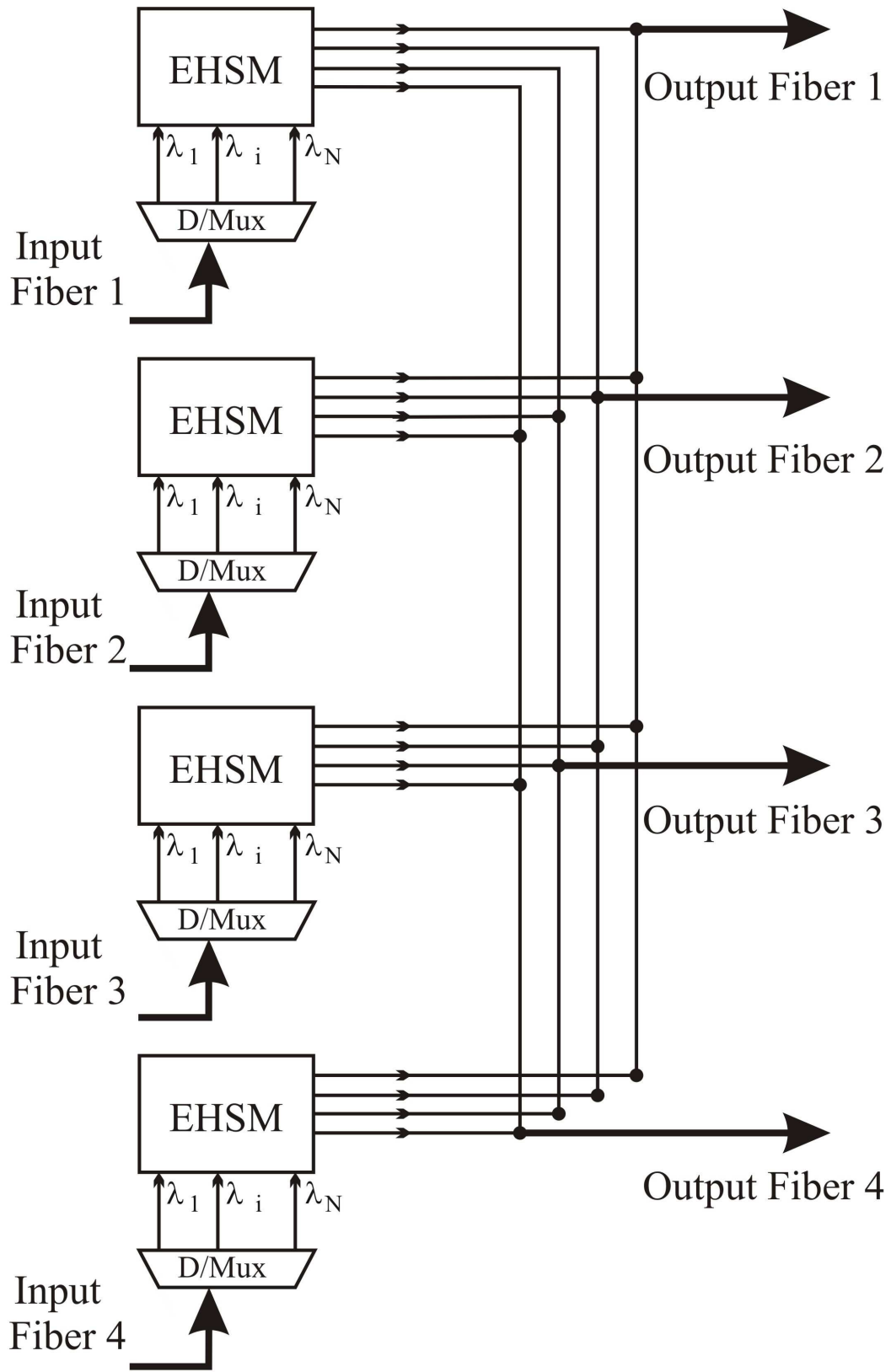


FIGURE 16. Electroholography based cross connect

The latter receives the wavelength channels in the form of a DWDM lightwave, demultiplexes them and performs the regeneration. It then regroup these channels into the input channel that transmits them back to the cross connect where they are redistributed to their final destinations. Thus, the EH based cross connect enables to limit the complex and expensive OEO operation only to the channels for which it is required.

3. Note that in the architecture illustrated in Figure 16 two channels of the same wavelength originating from two distinct input fibers may be allocated to the same output fiber. In this respect this architecture is 'blocking'. The system manager can avoid this situation when allocating the single wavelength channels to the output ports. It can also be avoided by the incorporation of wavelength conversion in a similar way to the incorporation of the regeneration operation as described above. Here as well the incorporation of wavelength conversion is cost effective as it is limited to the level that is statistically anticipated by the system designer.

4. The incorporation of optical amplifiers in the EH based cross connect is simple since each of the EHSM has power management capabilities.

Conclusions

WDM and in particular dense WDM have dramatically improved the capability of the ‘long haul’ segments of the networks to sustain a tremendous growth in data traffic. It is now well established as the reigning technology for point-to-point links in the capable of sustaining hundreds of Gigabits per seconds in a single fiber. However, the use of DWDM technology in the optical networks is limited to ‘long haul’ segments where it provides extremely efficient and cost effective point-to-point links. EH can supply the platform for viable wavelength selective switching technology that will enable to intelligently integrate the isolated disparate WDM point-to-point links into cohesive agile networks.

References

1. A. J. Agranat: Electroholographic Artificial Neural Networks, *Physika A* **200**, pp. 608-612 (1993).
2. A. J. Agranat: The Concept of Electroholography and Its Implementation in KLTN crystals, in *Proc. of OSA Topical Meeting on Spatial Light Modulators*, S. C. Esener (Ed.) (Lake Tahoe Nevada 1997).
3. M. Balberg, M. Razvag, S. Vidro, E. Refaelli, and A. J. Agranat: Electroholographic neurons implemented on potassium lithium tantalate niobate crystals, *Opt. Lett.* **21**, 1544 (1996).
4. B. Pesach, G. Bartal, E. Refaeli and A. J. Agranat: Free Space Optical Cross-Connect Switch by Use of Electroholography, *Applied Optics* **39** 746 (2000).
5. H. Kogelnik: Coupled wave theory for thick hologram gratings, *Bell Syst. Tech. J.* **48**, 2909 (1969).
6. L. Solymar and D. J. Cooke: *Volume Holography and Volume Gratings*, (Academic Press, London 1981).
7. A. Yariv: *Optical Electronics*, Chapter 18: "Two-beam coupling and phase conjugation in photorefractive media" (Saunders College Publishing, Philadelphia, 4th edition 1991) pp. 637 – 668.
8. D. B. Nolte: Photorefractive transport and multi-wave mixing, in *Photorefractive Effects and Materials*, D. B. Nolte (Ed.), (Kluwer Academic Publishers, Boston, Dordrecht, London, 1995) pp. 1-66
9. L. Solymar, D. J. Webb, and A. Grunnet-Jepsen: *The Physics and applications of photorefractive materials*, (Clarendon Press Oxford 1996).
10. P. Yeh: *Introduction to photorefractive nonlinear optics*, (John Wiley and Sons, Inc. New York 1993).
11. J. E. Geusic, S. K. Kurtz, L. G. Van Uitret, and S. H. Wemple: Electro-optic properties of some ABO_3 perovskites in the paraelectric phase, *Appl. Phys. Lett.* **4**, 141 (1964).
12. A. J. Agranat, V. Leyva, and A. Yariv: Voltage Controlled Photorefractive Effect in Paraelectric $KTa_{1-x}Nb_xO_3: Cu, V$, *Opt. Lett.* **14**, 1017 (1989).
13. J. P. Wilde et al.: Electric Field Controlled Diffraction in Photorefractive Strontium Barium Niobate", *Opt. Lett.* **17**, 853 (1992).

14. A. J. Agranat, R. Hofmeister and A. Yariv: Characterization of a New Photorefractive Material: $K_{1-y}Li_yTa_{1-x}Nb_xO_3$, *Optics Letters* **17**, 713 (1992) .
15. C. H. Perry, R. R. Hayes, and N. E. Tornberg: Ferroelectric Soft modes and anti resonance behavior in KTN mixed crystals, in *Proc. Of the International Conf. On Light Scattering in Solids*, M. Balkanski (Ed.), Wiley, New York 1975) pp. 812 – 815.
16. A. J. Agranat, R. Hofmeister and A. Yariv: Potassium lithium tantalate niobate photorefractive crystals, **U. S. Patent 5,785,898**, (1998).
17. A. J. Agranat, R. Hofmeister and A. Yariv, 'KLTN A new Photorefractive Material for Holographic Data Storage and Optical Computing Applications', **U. S. Patent 5,614,129**, (1997).
18. R. Hofmeister, S. Yagi, A. Yariv, and A. J. Agranat: Growth and characterization of KLTN:Cu,V photorefractive crystals, *J. Cryst. Growth* **131**, 486 (1993).
19. A. J. Agranat, L. Secundo, N. Golshani, and M. Razvag: Wavelength Selective Photonic Switching in Paraelectric KLTN, *Optical Materials* **18**, 195 (2001).
20. G. Bitton, Y. Feldman, and A. J. Agranat: Dielectric Properties of Photorefractive KLTN crystals, *Ferroelectrics* **239**, 213 (2000).
21. F.H. Mok, G.W. Burr and D. Psaltis: *Opt. Lett.* **21**, 896 (1996).
22. B. Pessach, Eli Refaeli and Aharon J. Agranat: “Investigation of the holographic storage capacity of paraelectric KLTN”, **Optics Letters** **23** 642 (1998).
23. M. Puterkovky: “The photorefractive sensitivity and holographic storage capacity in KLTN and KNTN crystals”, The Hebrew University of Jerusalem M. Sc Thesis, A.J. Agranat (Thesis Adviser) (2001).
24. K. Blotekjaer: “Limitations on holographic storage capacity of photochromic and photorefractive media”, **Appl. Optics** **18**, 57 (1979).
25. L. Kazovsky, S. Benedetto, and A. Willner: *Optical fiber communication systems*, (Artech House, Boston London 1996).

Figure Captions

FIGURE 1. The electrically controlled Bragg grating. (a) In the latent state. (b) In the active state.

FIGURE 2. A Detailed description of the electrically controlled Bragg grating in the transmission symmetrical configuration.

FIGURE 3. A schematic description of a 1x2 electroholographic switch. (a) State 1: the input is connected to output 1. (b) State 2: the input is connected to output 2.

FIGURE 4. A qualitative description of the photorefractive process. (a) Formation of the interference pattern. (b) Generation of the free charge carriers. (c) The distribution of the trapped space charge. (d) The spatial modulation of the index of refraction (birefringence).

FIGURE 5. Experimental results of the diffraction efficiency vs. the electric field of a Bragg grating in the transmission symmetrical configuration in KLTN.

FIGURE 6. The basic Electroholography based device in the latent and active states.

FIGURE 7. An electroholographic switch module performing grouping, multicasting, power management, and data monitoring.

FIGURE 8. An electroholographic switch module performing the 'Add' operation.

FIGURE 9. An Electroholography based switch device in the reflection configuration in which is PDL and PMD free.

FIGURE 10. An element of the electroholographic switch module in which an implementation of the polarization diversity architecture is demonstrated.

FIGURE 11. The spectral response of an EH based switching device: — The diffraction efficiency of a sinusoidal grating; - - - The output power collected by the output collimator.

FIGURE 12. An EH based switching device in the 0-90° configuration.

FIGURE 13. The spectral response of an EH based switching device in the 0-90° configuration.

FIGURE 14. The temporal response of an EH based switching device: — The Applied electric field; The diffracted power at: — — $T=T_c+15^\circ\text{C}$; — · — $T=T_c+20^\circ\text{C}$; — .. — $T=T_c+30^\circ\text{C}$

FIGURE 15. Electroholography based dynamic optical add drop multiplexer.

FIGURE 16. Electroholography based cross connect.

Index

Bragg grating 1, 2, 4, 5, 12, 24, 36
Electroholographic cross connect 2, 31
Electroholographic switching 2
Electroholography 1, 2, 3, 8, 14, 17, 22, 29, 31, 34, 36, 37
Grouping 18
KLTN crystal 2, 12, 13, 15, 19, 20, 22, 25, 27, 34, 35
Multicasting 18
Power management 19